Wolfgang Baether, Stefan Zimmermann and Frank Gunzer*

Pulsed electron beams in ion mobility spectrometry

Abstract: Ion mobility spectrometry is a well-known technique used to analyze trace gases in ambient air. Typically, it works by employing a radioactive source to provide electrons with high energy to ionize the analytes in a series of chemical reactions. During the past ten years non-radioactive sources have been one of the subjects of interest in ion mobility spectrometry, initially in order to replace radioactive sources as a result of general security and regulatory concerns. Among these non-radioactive sources especially pulsed sources have recently been shown to additionally improve the analytic information provided by ion mobility spectrometers. In this review we will describe the progress regarding the application of pulsed non-radioactive electron sources in ion mobility spectrometry and show the recent analytical advances that have been achieved by using pulsed electron beams.

Keywords: analytical information; ion mobility spectrometry; non-radioactive electron sources; pulsed electron beams.

***Corresponding author: Frank Gunzer,** Physics Department, German University in Cairo, Entrance El Tagamoa El Khames, New Cairo City 11835, Cairo, Egypt, e-mail: frank.gunzer@guc.edu.eg
Wolfgang Baether: Research Unit, Draegerwerk AG & Co. KGaA, Moislinger Allee 52-56, D-23542 Luebeck, Germany
Stefan Zimmermann: Sensors and Measurement Technology, Institute of Electrical Engineering and Measurement Technology, Appelstrasse 9a, Leibniz University Hannover, 30167 Hannover, Germany

Introduction

Ion mobility spectrometry (IMS) is well known for fast detection of chemical compounds in air down to very low concentrations of a few micrograms per cubic meter. Introduced in the 1960s as an analytical technique to separate and analyze gas phase ions at atmospheric pressure (Eiceman and Karpas 2005), ion mobility spectrometers have been developed from fast, sensitive and portal detectors for illegal drugs, explosives, and chemical warfare agents in early stages (McDaniel and Mason 1973, Asbury et al. 2000, Ewing et al. 2001, Eiceman 2002, Makinen et al. 2010) over analyzers of non-volatile and labile samples via electrospray ionization-ion mobility spectrometry (ESI-IMS) (Tang et al. 2006, Jafari et al. 2011), introduced in the late 1980s to analyzers of metabolomes and proteomes if combined with mass spectrometry (McMinn et al. 1990, Wüthrich 1993, Chiarello-Ebner 2006, Eckers et al. 2007, Liu et al. 2007, McLean et al. 2007, Waltman et al. 2008, Djidja et al. 2009, Krueger et al. 2009, Armenta et al. 2011). In more modern applications, even the study of protein-protein and non-covalent protein-ligand complexes is possible (Ruotolo et al. 2008, Politis et al. 2010). Particularly as portable analyzers, ion mobility spectrometers exist in numbers and locations at present unparalleled by any other comparably sophisticated chemical analyzer (Borsdorf et al. 2011).

IMS-based detectors work by employing an ionization source that ionizes the sample in ambient air. These ions are then accelerated into a drift tube of a certain length (typically a few centimeters) where they collide with ambient air molecules. At the end of the drift tube the ions with different mobilities are separated, i.e., ions with high mobility reach the end of the drift tube faster than molecules with lower mobility. This drift time spectrum is the main analytical information provided by IMS. Because no vacuum sealing or pumps are necessary, the device can be reduced very much in size. The detector is, in general, a simple Faraday plate which can also be realized with small dimensions. The ion mobility spectrometer has thus three distinct sections: the reaction region (width: only a few millimeters) with the ionizing source; the drift region (width: circa 5 cm) for the separation of the analyte ions according to their mobilities; and the collector region (width: again, only a few millimeters) with the Faraday plate. The diameter of the tube with these three sections is typically only a few centimeters.

The flow of the ions is controlled with the help of electric fields. In a typical set-up, there is a constant field present in the reaction region and the drift region (the magnitude might even be the same in both regions, which simplifies the set-up) that accelerates the ions after their production towards the detector. Because the source produces ions continuously, a pulsed gate opens for a certain time between the reaction

region and the drift region and thus allows ion pulses with a certain temporal width and at a certain frequency to reach the detector. This gate is typically a Bradbury-Nielsen ion gate, a set-up of parallel interleaved wires having their plane perpendicular to the ion beam's propagation direction (Bradbury and Nielsen 1936). If the potential difference between neighboring wires is zero, the gate is open because the ion beam can pass it undeflected; a closed gate is realized by applying a certain voltage with different polarity to each neighboring wire pair so that the ion beam is deflected by a voltage-dependent angle and so does not reach the detector. Bradbury-Nielsen gates are compact and allow for fast switching times and thus short ion pulses.

An alternative to using a Bradbury-Nielsen gate is to use a weak electric field of only a few V/cm during the ionization in order to prevent the drift of ions into the drift region. At a frequency of, e.g., 30 Hz, a voltage pulse called the extraction pulse of about 1000 V/cm and a few hundred microseconds' duration accelerates the ions into the drift region, where they collide with the air molecules. Inside the drift region a constant field of about 200 V/cm leads to a mobility dependent drift velocity and thus to the separation of the species.

At the end of the drift region, a constant field of, again, about 1000 V/cm accelerates the ions towards the Faraday plate where they create the signal. The longer the drift regions, the better the different species can be separated via their drift times, but this limits then the portability of the device. In order to increase the separation, the ions collide with a flow of ambient air (typically a few hundred ml/min) that is propagating against the direction of the ions. Figure 1 illustrates a general IMS device set-up and the applied voltages.

For reasons of simplicity, the ionization source in most commercial devices is a radioactive substance: mainly ^{63}Ni, but also ^{241}Am and ^{3}H. The different sources ionize with different energies: ^{63}Ni emits electrons with a maximum energy of 67 keV and an average energy of 17 keV; ^{241}Am emits short-range alpha particles at over 5.4 MeV; ^{3}H emits electrons at less energy than ^{63}Ni with a maximum value of 18.6 keV and an average value of 5.7 keV (Guharay et al. 2008). They produce so-called reactant ions via a sequence of reactions, especially with N_2. The reactant ions are positively charged water clusters or O_2^- clusters. These ions ionize *via* charge transfer reactions the analyte (Eiceman and Karpas 2005). Since the emission of particles by the radioactive source is a continuously ongoing process, the formation of analyte ions is therefore also continuous. The polarity of the field/extraction pulse that accelerates the ions into the drift region selects either the positively charged ions or the negatively charged ions out of all the ions present in the reaction region, and so the device is said to be operated in either the positive mode or the negative. Certain substances are better detected or even only detected in the positive mode. In the negative mode the analytes are adduct ions between the sample and hydrated O_2^-; in the positive mode there exist protonated monomer molecules and furthermore, depending on the analyte and its concentration, proton-bound dimer molecules. An IMS spectrum shows in either mode at least one peak that is formed by the reactant ions. This peak is called the reactant ion peak (RIP). The RIP has in general the highest mobility and correspondingly the fastest drift time; the analyte ions have normally a lower mobility and so a longer drift time compared to the RIP (Figure 2), but exceptions do exist.

From the drift times the mobility can be calculated. Because this quantity depends on certain ambient parameters, the so-called reduced mobility is normally used, which is the mobility normalized regarding temperature and pressure to ambient conditions. The obtained values range from ca. 1.2 $cm^2V^{-1}s^{-1}$ to 2.2 $cm^2V^{-1}s^{-1}$, with an accuracy no better than 0.01 $cm^2V^{-1}s^{-1}$. Therefore peak overlap or even similar reduced mobilities for different substances are probable, and the substance identification based on

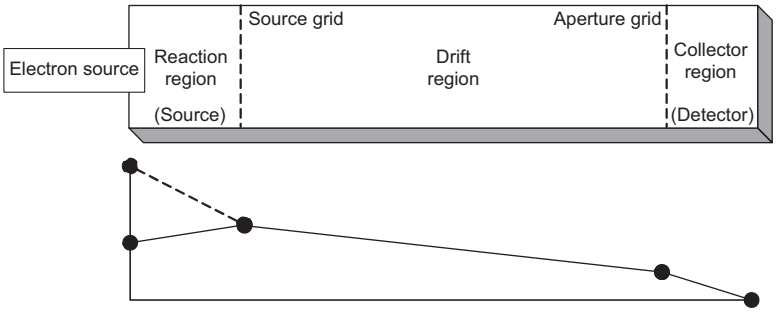

Figure 1 Typical set-up of an ion mobility spectrometer with its three sections (upper drawing). In the reaction region, the analyte molecules are continuously ionized. Electric fields accelerate the ions with a certain frequency into the drift region, which they cross with different flight times because of their different mobilities in air. In the collector region, a detector forms the signal proportional to the amount of ions. The lower graph illustrates the voltages applied to each section.

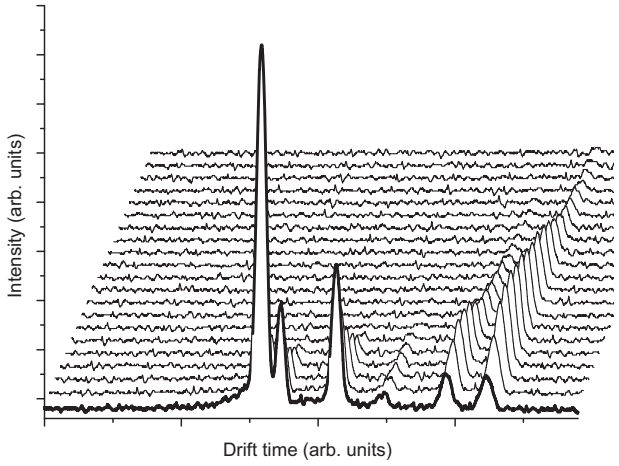

Figure 2 Typical IMS spectrum, shown for a mixture of dimethyl methylphosphonate (DMMP) and dimethylformamide (DMF). The six peaks (from left to right) are RIP, DMF monomer, DMMP monomer, DMF dimer, DMMP+DMF asymmetric dimer, DMMP dimer. Furthermore, it is shown how the spectrum changes if a pulsed source is used and the delay time between ionizing electron pulse and ion extraction (with subsequent detection) is increased (each spectrum was recorded 300 µs after the previous one).

the mobility alone is likely to lead to misinterpretation (Eiceman and Karpas 2005). Ion mobility spectrometry is fast (response time only a few seconds), sensitive (detection of substance concentrations of lower parts per billion (ppb), or in certain cases even parts per trillion (ppt) are possible), simple in effort and maintenance, and portable. The analytical information, especially the selectivity, is, however, quite limited. Successful approaches trying to improve the situation, with special focus on the resolving power of IMS devices, concentrated especially on the electron source and the voltage schemes applied to the device. Regarding the electron source, prominent examples are electrospray ionization (typically for liquid samples) (Wittmer et al. 1994, Chen et al. 1996, Wu et al. 2000, Harris et al. 2008, Yamagaki and Sato 2009), optical sources (high-intensity light sources resp. laser, X-ray) (Matsaev et al. 2002, Sielemann et al. 2002, Oberhüttinger et al. 2009), corona discharges (Tabrizchi et al. 2000, Schmidt et al. 2001, Khayamian et al. 2003, Han et al. 2007, Mulugeta et al. 2010, Tabrizchi and Ilbeigi 2010), and electron guns (Gunzer et al. 2010a). These sources were also examined in order to have non-radioactive alternatives because of the technical, organizational and related financial complications that accompany the application of radioactive substances. Regarding the voltage schemes, in particular high-field asymmetric field ion mobility spectrometry (FAIMS) (Klaassen et al. 2009, Shvartsburg et al. 2009, Schneider et al. 2010, Barnett and Oullette 2011) has attracted a lot of interest in recent years.

In general, the non-radioactive electron sources work continuously, like the radioactive sources that they try to replace. Only the corona discharge source and the electron gun have been successfully applied in a pulsed mode (Figure 3). This review therefore describes the development of the application of pulsed corona discharges and electron beams in ion mobility spectrometry in the past 10 years. These years can be separated into two phases: from 2001 to 2005 only pulsed corona discharge sources have been investigated, and since 2010 only pulsed electron guns. While the corona discharge sources were only investigated regarding their potential to replace their radioactive non-pulsed counterparts, the application of pulsed electron guns has been shown to additionally offer further analytical information. This review will therefore first characterize the pulsed corona discharge and describe its application and benefits for ion mobility spectrometry. It will then characterize and describe the pulsed electron gun with its progress regarding analytical information that can be obtained from pulsed ion mobility spectrometers.

Pulsed corona discharge

A continuously working corona discharge-based source was investigated regarding its usefulness for IMS by Tabrizchi et al. (2000). Although it was initially intended only to

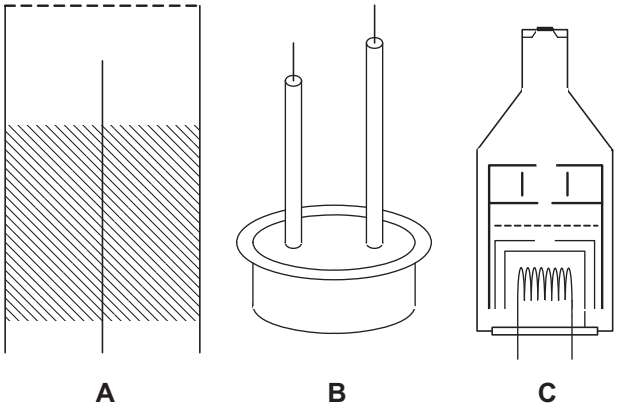

Figure 3 Different electron sources which have been used in a pulsed manner in IMS. Pulsed corona discharge in a point-to-plane configuration (A). The electrodes are in the center and at the outer housing. Without the mesh at the top it would be a point-to-ring configuration, which was actually the first ever used pulsed source. Pulsed corona discharge between two electrodes (B) and free electron beams produced by a glowing filament inside a vacuum tube (C). With the help of electrical fields the electrons are accelerated through a ceramic foil serving as an exit window at the top of the tube.

be a non-radioactive alternative, the corona discharge source showed greatly improved ionization efficiency and thus signal intensity as well as signal-to-noise-ratio. Also, additional peaks appeared in the ion mobility spectrum obtained (Borsdorf and Rudolph 2001). These peaks are the result of a different ion chemistry when using high-energy discharges, which is a drawback because the ideal replacement source should lead to the same, well-understood chemical reactions as those obtained with radioactive sources. The first reported pulsed corona discharge (Xu et al. 2001) was intended to be used in miniature IMS devices where the small dimensions would not allow storage of a high number of ions, and thus a continuously working corona discharge source would mean a significant loss of ions and waste of resources. This idea of increased efficiency was also the main motivation for Hill and Thomas (2002, 2003, 2005) and An et al. (2005), specifically energy efficiency, who described different versions of pulsed corona discharge-based sources in IMS spectrometers.

Characterization of the source

The first pulsed corona discharge was described at the Sixth International Workshop for Ion Mobility Spectrometry in Germany by Clark et al. (1997). However, the first journal paper describing a pulsed corona discharge was written by Xu et al. (2001), who used the same source in a later publication (Xu et al. 2003). It consisted of a Ni corona tip with a radius of approximately 25 µm. Together with the IMS device's housing this tip formed a tip-ring configuration. Voltage pulses of 1–3 kV with a width between 400 ns and 400 µs were applied with a frequency of 20 Hz. The 2003 article described the same set-up in more detail. The distance between the tip and the ring in that set-up varied from 0.5 mm to 3 mm, but a stable corona discharge required a distance of greater than 1.96 mm. The pulse length varied from 40 ns to 100 µs. The reported resolving power was 13 (drift tube width 2.5 mm, drift tube length 47 mm; a good resolving power in IMS devices is 40 and better), with a maximum signal-to-noise ratio of 35. Because of the short pulse duration they used no gate (e.g., Bradbury-Nielsen gate) between the reaction region and drift region. The positive mode IMS signal saturated with a pulse width larger than ca. 1.2 µs, which depended on the corona potential and could be as low as 0.5 µs. In the negative mode, the signal strength was reduced with longer pulse duration, reaching a reduction of ca. 40% at a pulse duration of 85 µs.

Hill and Thomas (2002, 2003, 2005) described another set-up employing a pulsed corona discharge. They used two electrodes 4 mm apart, one 16.5 mm long and one 13 mm long, both having a 3 mm long gold wire as a tip with a diameter of 10 µm (in 2005: 50 µm diameter). Instead of single pulses, a sequence of pulses was applied to the electrodes with decaying amplitude. The frequency was 82 kHz, the initial amplitude ca. 2 kV, and the duration of the whole pulse train was approximately 1000 µs. After the ionization the ions drifted down the 8 cm wide reaction region, and 12 ms after the ionization pulse the ions were injected into the similarly 8 cm long drift tube, which was separated by a Bradbury-Nielsen gate from the reaction region. The resolving power, though not directly reported but obtainable from the published graphs, was 39.

A third set-up has been described by An et al. (2005). Instead of a point-to-ring configuration, as used by Xu et al. (2001, 2003), they used a point-to-plane configuration, where a copper electrode of 0.4 mm diameter was located at a distance of 6 mm from a stainless steel mesh electrode of 14 mm diameter. The voltage pulse that created the corona discharge measured 8.5 kV in amplitude and 500 ns in duration, repetition rate 20 Hz. Used in an IMS spectrometer with a 65 mm long drift tube of 40 mm diameter which was not separated by any form of gate from the reaction region, they achieved a resolving power of ca. 21.

Application of the pulsed corona discharge

All three previously described pulsed corona discharge sources were primarily developed in order to replace the standard radioactive source with a non-radioactive one. Corona discharge sources had been found to be a suitable candidate, and using them pulsed should lead to improved energy efficiency. Correspondingly, the sources were investigated regarding their potential of reproducing IMS spectra obtained with radioactive sources. The additional possibilities arising when using pulses of different intensity and duration were only marginally of interest, and the ability to use a time delay between ionization and ion detection to investigate the temporal development of the ions was not part of the studies all. Therefore the first spectra described by Xu et al. (2001, 2003) obtained with the ring-tip configuration showed only the peaks obtained for air, in this case with N_2 as drift gas. Normally, only the RIP should appear in the spectrum, so that a comparison regarding resolving power and peak intensity would be possible. While in the negative mode only one peak was indeed observed, it was two in the positive mode. Besides the RIP ions (protonated water clusters), an additional peak caused by $(H_2O)_n(N_2)_mNH_4^+$ clusters (n=0,1; m=0–3) appeared, probably because of the drift gas being N_2; the

presence of NH_4^+ is not unusual for RIP ions. However, in the case of continuously operating corona discharge sources it was already known that this source leads to a different set of reactant ions and so also to different ionization mechanisms for the analyte (Eiceman and Karpas 2005). Further investigations by Xu et al. (2001, 2003) concentrated on optimizing the source regarding the applied voltages; dependencies on the pulse width were only investigated to gain some insight into the ionization mechanism.

The challenges of using a corona discharge as a replacement for the radioactive sources arising from of different ionization chemistries was also described by Hill and Thomas (2003). Especially the production of O_3 when increasing the corona energy and the multitude of related side-reactions required technically challenging stable and reproducible sources; the formation of NO_2^- and NO_3^- related cluster ions and the subsequent quenching of product ions seemed to make the corona discharge in general unsuitable for the negative mode. Therefore they described their two-electrode set-up which could be used in both positive and negative mode. Their studies then concentrated on showing how well the source performed when recording spectra of ambient air with a subsequent mass-spectrometric analysis of the RIP. The result was that at least in the positive mode the obtained ions are the same as those obtained with a ^{63}Ni source [although Borsdorf and Rudolph came to a different conclusion 2 years earlier (Borsdorf and Rudolph 2001)], while in the negative mode enough O_2^- ions are obtained to produce analyte ions in sufficient quantities (so leading to a sufficiently strong analyte signal), but the reactant ion chemistry is more complicated with this source than when using ^{63}Ni because of the presence of NO_3^- in particular.

Hill and Thomas subsequently investigated the influence of delaying the extraction of the ions from the reaction region (Hill and Thomas 2005). This was the first time that the additional options which a pulsed source offers (i.e., control over the ionization event in terms of intensity, duration, and delay of ion extraction and detection) were discussed; in previous papers these possibilities were only briefly mentioned because the focus was on establishing if, simply speaking, the pulsed source leads to the same spectra as the radioactive sources. Here it was described how, by varying the delay before the ions are extracted from the reaction region and injected into the drift region, it should be possible to investigate the dynamics and kinetics of the ionization processes. Different parts of the product ions could be selected, which also undergo further equilibration processes during the delay. Hill and Thomas (2005) even speculated that it should be possible to tune a system and thus enhance the selectivity because of this selection of ions. The actual investigation, however, concentrated on using different delays between ionization and ion detection (between 10 and 20 ms; lower delay times were probably not possible because of the large reaction region that had to be crossed drifting, leading to a first separation of ions, before reaching the drift tube) in order to further separate the different ion species and thus to better analyze the formation process with subsequent mass spectrometric analysis.

Also in 2005, An et al. published their study on the development of a short-pulsed corona discharge ionization source for IMS (An et al. 2005). The main goal was here again using the pulsed corona discharge as a non-radioactive source with low-energy consumption in a miniature IMS device, but with an additional advantage of simplifying the IMS device's set-up because no special means were necessary to separate the drift tube from the reaction region (i.e., no electrical or mechanical set-up necessary to extract ion pulses from the extraction region where ions are continuously being produced when using a non-pulsed source) and thus being beneficial regarding miniaturizing IMS devices. The study concentrated on characterizing the source (e.g., influence of peak voltage of the pulse on peak current for different distances between electrode and mesh, and for different electrode diameters), and on the application as an ionization source for IMS, showing an IMS spectrum of acetone and demonstrating the stability of the source (mean signal intensity 2.9 nA with standard deviation of 0.14 nA, mean IMS peak position 8.6 ms with standard deviation of 0.08 ms).

Pulsed electron gun

Although the use of pulsed ionization sources was hypothesized to improve low selectivity in IMS (Hill and Thomas 2005), it was not successfully demonstrated until 5 years later by our group. A number of experiments showed that using a pulsed source and the investigation of the decay of ions in the reaction region offers additional analytical information beyond the reduced mobility, which is the only parameter that can be obtained with standard IMS devices. The electron source used in these experiments was not a pulsed corona discharge, but a pulsed electron gun. Electron guns based on vacuum tubes are known since the 1890s and have experienced various improvements. The challenge in IMS is not producing the electron beams (the internal set-up of electron guns has been for a long time, and still is, a simple glowing filament with

a set of electrodes to create a controlled beam of free electrons), but to create an electron beam of sufficient intensity outside the vacuum tube. This requires an exit window that is stable enough to uphold the vacuum inside the tube without leading to a high loss of electrons when they penetrate the window. A suitable device has been developed by (Wieser et al. 1997), which has been applied, for example, in plasma experiments and other analytical chemistry-related applications (Mühlberger et al. 2005, Morozov et al. 2006, 2008a,b). The following part describes this source and its application in IMS spectrometers, together with the innovative analysis of IMS signal decay curves.

Characterization of the source

The electron gun used in these experiments is a small glass tube that ends in a source punch of 10 mm diameter. An exit window for the free electrons produced inside the tube is located at the end of the punch. This window is a 0.5 mm^2 ceramics foil made of 300 nm thick silicon nitride. Electrodes inside the tube allow creating electron beams of up to 12 keV, which are accelerated from the vacuum inside the tube (better than 10^{-6} mbar) through the window. After passing the window, the electrons reach a kinetic energy distribution similar to that of a ^3H source. With the help of the accelerating voltage and the electrodes, as well as the voltage supplied to the glowing filament, the intensity of the beam can be varied, so that the obtained IMS signals (e.g., RIP) can achieve a 10-fold increase in their intensity. Signal-to-noise ratios in such a set-up using a standard IMS tube reach 80, the resolving power (5 cm long drift tube not using a gate between the reaction region and drift region, but a weak field in the reaction region during ionization instead) is ca. 40. The electron pulses can be varied regarding their duration from 1 to 100 µs, and good signals are already obtained with 10 µs pulses (Gunzer et al. 2010a).

Application of the pulsed electron gun in IMS

Simple comparison of spectra in the first experiments described in 2010 showed that the pulsed electron gun leads to similar spectra to those obtained with a radioactive (^3H) source. The ^3H source leads to free electrons of similar average kinetic energy, so that no additional side-reactions are triggered as, for example, in the case of corona discharges. Measuring the ion signal intensity dependence on the delay time between ionization and ion-extraction from the reaction region into the drift region showed that the signal intensity in general decreases with increasing delay time, although also an initial increase and subsequent decay can be observed. Therefore with a certain delay time, certain substances which decay faster can be filtered out, so that only substances which decay more slowly remain in the spectrum (Gunzer et al. 2010b). The selectivity is thus increased regarding these long-living analytes. A major problem for IMS applications outside controlled conditions is humidity, which has a huge influence on IMS signals because it directly affects the production of analyte ions (as a result of the dependence of the reactant ions on water and water clusters). The normalized decay curves of the RIP, however, showed that humidity might influence the signal intensity, but the decay is independent from humidity levels. Thus not only the selectivity benefits from the pulsed operation, but possibly also the field performance.

A following study concentrated on establishing the influence of different parameters on the RIP's decay curve: on the one hand to further explore the possible advantages of the pulsed operation and of the decay curves; on the other hand to help clarify what is responsible for the decay (Baether et al. 2010). Two options seemed possible: gas phase recombination reactions, and collisions with the housing leading to a discharge of the ions. Especially the latter case would mean that the decay curves would offer no additional, orthogonal information, because then the decay would depend on how fast the analyte ions reach the housing, which would depend on their drift velocity inside the reaction region (caused by electric fields which are always present and normally used to prevent an early drift of the ions into the drift region). In a study investigating how the different voltage parameters influence the decay curves, it was shown that increasing the electrical field strength during the delay inside the reaction region leads to a faster decay. Although these fields are very small (3–15 V/cm), they reduced decay times in the curves by up to twofold. However, a direct, general proportionality of the drift velocity with respect to the electrical field strength could not be calculated from the data; such proportionality is necessary should the drift to the housing be responsible for the decay, because the drift velocity is known to be proportional to the field strength (Eiceman and Karpas 2005). Furthermore, neither the intensity nor duration of the electron pulse had an influence on the decay curve, so the decay characteristic is quite stable with respect to external influences.

The next step was to analyze the decay curves of certain analytes. Two papers concentrated on dimethyl

methylphosphonate (DMMP) (Gunzer et al. 2011) and toluene diisocyanate (TDI) (Baether et al. 2012a). DMMP is well known among the IMS community, since it is a simulant substance for the nerve gas Sarin (GB); because of the importance of IMS for chemical warfare agent detection, DMMP has been investigated in a number of papers (Steiner et al. 2005, Davis et al. 2009). The typical strong analyte signals obtained with standard IMS are also obtained with a pulsed IMS. The decay curves, however, showed a strong dependence on the analyte concentration. With standard IMS, the analyte concentration changes the intensity of the analyte signal, or to be more precise, the ratio of the RIP's signal intensity and the analyte's signal intensity. Since the analyte is ionized in charge transfer reactions with the reactant ions, the RIP intensity decreases when the analyte's intensity increases. The decay curve obtained with the pulsed IMS changed more than just the intensity. It was observed that with lowering the concentration, the decay curve changes from a pure exponential decay, with slower decay towards lower analyte concentrations, to an initial increase followed by an exponential decay after reaching a certain maximum intensity. Lowering the concentration further leads, then, to a lower initial intensity compared to the maximum intensity, to a shift of this maximum intensity towards longer delay times and to a slower decay after reaching the maximum intensity. So lowering the concentration shifts the whole decay curve towards longer delay times. Also, these decay curves decay faster if the strength of an electrical field present during the decay is increased.

DMMP is measured in the positive mode of the IMS. Typical for that mode is that not only peaks related to the analyte ions (monomers) are observed, but also peaks formed by symmetric proton-bound analyte dimers (Ewing et al. 1999, Jazan and Tabrizchi 2009). Since the monomers contribute to the dimer formation, there is a complex relationship between these two peaks' intensities. In general, from a certain analyte concentration on, not only the monomer signal appears but also the dimer signal. Increasing the concentration leads then to a stronger dimer signal and a weaker monomer signal, and from a certain concentration on, only the dimer signal is visible in the spectrum. For DMMP, both signals show the same dependence of the decay curve on the analyte concentration as described before, but the monomer signal needs a much lower concentration to show an initial intensity increase with respect to the delay time instead of a pure exponential decay (Figures 4 and 5). The dimer signal is at these concentrations already shifted to very long decay times, the initial intensity (delay time t=0 ms) possibly even zero, i.e., only at a longer delay time the dimer signal

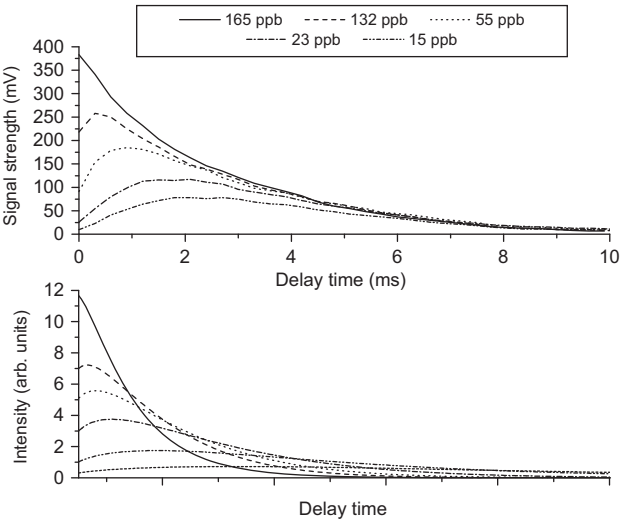

Figure 4 Comparison of measured (upper graph) and calculated (lower graph) signal intensities for a dimer signal (measurements shown for ethyl methyl ketone).

reappears in the spectrum. The concentration-dependent behavior of the decay strongly supports the assumption that the decay is caused by gas phase recombination reactions, because drift times towards the housing should not be affected by a change of analyte concentration. A further hint towards recombination reactions was also reported in the same paper, showing that the decay behavior of the RIP changed when the general composition of ions in the reaction region was altered by adding 1,2-dibromoethane, which forms negative ions in IMS devices.

TDI is, in contrast to DMMP, investigated using the negative mode of the IMS (Brokenshire et al. 1990, Roehl 1991). One major consequence is that in this mode no dimer

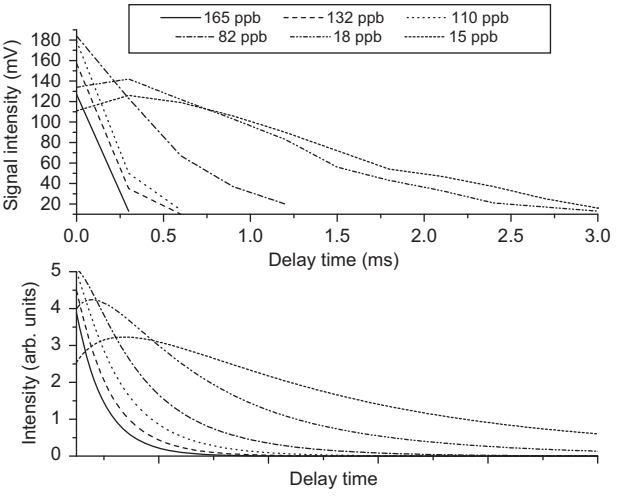

Figure 5 Comparison of measured (upper graph) and calculated (lower graph) signal intensities for a monomer signal (measurements shown for ethyl methyl ketone).

signals are formed, so the relationship between the signal intensities is much simpler. A study concentrating on TDI was conducted in which the main goal was to investigate whether pulsed IMS can be used as a TDI detector regarding the sensitivity (sufficient signal strength at concentrations below 5 ppb required) in combination with the other positive aspects of the decay curves. One major result was that for TDI even at concentrations as low as 2.5 ppb the decay curves show the same behavior as DMMP regarding change of concentration (i.e., shift to longer delay times with lower concentrations) with sufficient signal intensities. Furthermore, again the decay behavior showed almost no dependence on the humidity. Especially in the negative mode humidity and the related water molecules are problematic for IMS measurements, leading to a drastic reduction in signal intensity (Eiceman and Karpas 2005, Makinen et al. 2011). TDI showed almost no dependence on the humidity in the absolute signal intensities, while phenyl isocyanate, for example, suffered a drastic maximum intensity reduction of 80% when increasing the humidity from 0% rh to 50% rh. However, in the normalized curves, both substances showed almost no influence of the humidity, i.e., the decay itself is only slightly influenced by humidity changes, even if the absolute intensity changes drastically.

Analytical Information extracted from decay curves

TDI and DMMP showed in their decay behavior that more information is available when using the pulsed electron source than just the reduced mobility. Further studies concentrated on these additional parameters obtainable from the decay curves. The dependence of the decay on the analyte concentration seemed particularly interesting, because it addresses one of the main problems in IMS, i.e., not being able to measure quantitatively. In theory, because of the charge transfer reactions between reactant and analyte molecules and the conservation of charge, it should be possible to estimate the analyte concentration from the ratio of the RIP's intensity and the intensity of the analyte's peak (Garofolo et al. 1996, Khayamian et al. 2001, 2006, Eiceman and Karpas 2005). In reality, such an approach suffers from great fluctuations in the signals, and variations of up to 25% have been reported (relative standard deviation for peak areas, see Poziomek and Eiceman 1992). Advanced techniques like specialized statistical approaches or even computer algorithms like artificial neural networks have been applied in order to improve the reliability of extracting the analyte concentration from the peak intensities (Boger and Karpas 1994, Zheng et al. 1996, Fraga et al. 2009). All of these approaches, however, depend on the quality of data that they are supplied or trained with. Because the decay curves are quite stable with respect to external parameters, and because their decay characteristic depends on the analyte concentration, a study was conducted to determine the details of this dependence on the analyte concentration (Baether et al. 2012b). Besides DMMP and TDI, two more substances were investigated, ethanol and ethyl methyl ketone. Only the decay behavior should be used to obtain quantitative information, so decay curves normalized with respect to the maximum intensity were investigated. The results showed that it is indeed possible to extract the analyte concentration from the normalized decay curve, with a precision of better than 5 ppb in all investigated cases regarding signal fluctuations. One restriction is the range over which decay curves allow for the determination of this parameter, which is substance specific (ethanol showed the smallest range with 5–65 ppb, and ethyl methyl ketone showed the largest with 20–165 ppb). The range depends on which type of signal is used (in the positive mode: monomer or dimer), and how the information is extracted. If the concentration is low enough, the decay curve has three distinct parts: the initial increase of intensity towards the maximum intensity; the location of the maximum intensity; and the decay after reaching this maximum intensity. Especially the onset of the initial increase, i.e., the relative intensity at a delay time of t=0 ms, went lower when the concentration was lowered. If the concentration is too high, the decay curve immediately decays exponentially, and then there is no initial increase. If the concentration is too low, the onset of the initial increase remains zero at delay t=0 ms. The location of the maximum intensity (i.e., its delay time) shifts to longer delay times with lower concentrations, but this shift is not very strong (Figures 4 and 5). The decay after reaching the maximum is slower with lower concentration. There are two simple possibilities to use these dependencies on the concentration: either observing the delay time necessary to reach a certain intensity ratio; or to observe the intensity ratio at a fixed delay time. Both possibilities have been employed, and especially using the intensity ratio at a fixed delay time t=0 ms seemed suitable, but it then suffered from the limited concentration range described before. Using a fixed intensity ratio after reaching the maximum intensity, e.g., delay time when the signal intensity dropped to 50%, also yielded a good parameter to determine the concentration, although the change of this parameter was quite low at higher concentrations. The general observation was that both curves

change only little at certain higher concentrations (or not at all anymore in the case of using the intensity at t=0 ms delay), so this fact determines the upper concentration limit in order to reach a certain precision (in this study, better than 5 ppb). Towards lower concentrations the absolute intensities of the curves become low and thus the error due to fluctuations becomes relatively stronger, and this correspondingly puts the lower concentration limit. But within their ranges these parameters allow for stable concentration estimation that then can support other intensity-based approaches as mentioned before.

Another interesting behavior of the decay curves was observed when mixtures of two substances were analyzed. The original goal was to see if the decay behavior changes and how the substances influence each other. Certain pairs which show monomer and dimer signals have been investigated with different concentrations for each of the partners: ethanol and ethyl methyl ketone, ethyl methyl ketone and DMMP, and DMMP and dimethylformamide. The proton affinities of these substances are 776.4 kJ/mol (ethanol), 827.3 kJ/mol (ethyl methyl ketone), 898.4 kJ/mol (DMMP) and 887.5 kJ/mol (dimethylformamide). Thus the influence of the proton affinity on the decay behavior should become apparent. The results were that the monomer signals decayed exponentially very fast, in general faster than in the case when only a single substance is present in the IMS device. Furthermore, both monomer signals decayed in a similar fashion. The relative concentration (i.e., higher for the one partner or the other) did not have an influence on this behavior. The dimer signals, however, behaved differently. They decayed much more slowly compared to the monomer signals, or even showed first an increase in intensity and then a decay (Figure 6). As a result of this behavior, it was possible to remove the monomer signals completely from the IMS spectrum with a relatively short delay. The decay itself was influenced by the relative concentration (i.e., was dependent on which partner was present in a higher concentration), but the partner with the higher proton affinity was always the substance with the slowest decay, i.e., with a certain long delay time it was possible to remove all signals from the IMS spectrum except the dimer signal of the partner with the higher proton affinity. This longer decay of the substance with higher proton affinity was furthermore observed by Cochems et al. (2012) for a mixture of 1-octanol (proton affinity 846. kJ/mol) and DMMP. This influence of the proton affinity is a further hint towards gas phase recombination reactions as the main reason for the signal decay.

It becomes clear that the application of a pulsed electron source and the corresponding recording of the signal

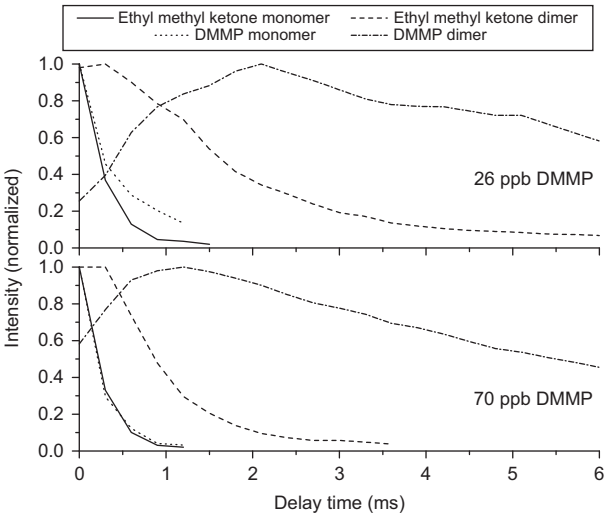

Figure 6 Dimer and monomer signals decay differently in mixtures, here shown for DMMP and ethyl methyl ketone (concentration 110 ppb). The dimer signals decay much more slowly, and the dimer of the substance with the higher proton affinity (DMMP) decays most slowly even if its concentration is low compared to the other substance's concentration.

decay with respect to the delay time between ionization and ion detection yields further analytical information for IMS. The original, continuously working set-up allows only for the determination of the reduced ion mobility. As described in the introduction, IMS devices have typically a low resolving power of not better than 0.01 $cm^2V^{-1}s^{-1}$, with the reduced mobilities ranging typically from 1.2 $cm^2V^{-1}s^{-1}$ to 2.2 $cm^2V^{-1}s^{-1}$. Therefore using the reduced mobility alone for substance identification might lead to misinterpretation. The pulsed operation provides in this case further information, because it allows for a discrimination of monomer and dimer signals, and furthermore to estimate the proton affinity (e.g., if a substance with known proton affinity is investigated together with an unknown substance). In summary, pulsed operation increases the selectivity (i.e., via the delay time certain signals can be filtered out), the identification power (via discrimination of monomer and dimer signals, and allowing for an estimation of the proton affinity) and offers improvement for quantitative measurements in the lower ppb range.

Simplified reaction model

While the initial signal decay led to the assumption that either gas phase recombination reactions or collisions with the housing could be responsible for the decay, its dependence on the concentration and the proton affinity shifted the focus strongly towards accepting

recombination reactions as the dominant process. With help of a simple rate constant approach based on basic recombination reactions (involving only positive and negative RIP ions, as well as negative analyte ions) a qualitatively correct signal decay could be mathematically reproduced for the negative mode (TDI, Baether et al. 2012a) including its dependence on, for example, electrical field strength and analyte concentration. For the positive mode, this model has to be extended by including the dimer formation. The proton-bound dimer is formed by reactions of analyte monomers with neutral analyte molecules and recombines with the negative RIP ions, decomposing into two neutral analyte molecules. The reaction equations for the complete decay become then:

$$RIP^+ + A \xrightarrow{k_1} RIP + A^+$$

$$RIP^+ + RIP^- \xrightarrow{k_2} 2RIP$$

$$RIP^- + A^+ \xrightarrow{k_3} RIP + A$$

$$A^+ + A \xrightarrow{k_4} A_2^+$$

$$RIP^- + A_2^+ \xrightarrow{k_5} RIP + 2A$$

$$\frac{d[A]}{dt} = -k_1[RIP^+][A] + k_3[RIP^-][A^+] - k_4[A^+][A] + 2k_5[RIP^-][A_2^+]$$

$$\frac{d[A^+]}{dt} = k_1[RIP^+][A] - k_3[RIP^-][A^+] - k_4[A^+][A] - k_6[A^+]$$

$$\frac{d[RIP^-]}{dt} = -k_2[RIP^-][RIP^+] - k_3[RIP^-][A^+] - k_5[RIP^-][A_2^+]$$

$$\frac{d[RIP^+]}{dt} = -k_1[RIP^+][A] - k_2[RIP^-][RIP^+]$$

$$\frac{d[A_2^+]}{dt} = k_4[A^+][A] - k_5[RIP^-][A_2^+] - k_7[A_2^+]$$

Taking just the recombination reactions into consideration leads to decay curves which do not reach zero for the dimer. Furthermore, it is difficult to simulate the influence of the electrical field with these equations only. Therefore an additional loss mechanism was introduced. Based on the observation that the signal decay time constant scales nearly linear with the field strength in the reaction region (very well visible for DMMP (Gunzer et al. 2011), for TDI the linearity is less), this loss term was formulated as $d[B^+]/dt = -k[B^+]$ with B being the monomer or dimer ions, and k being k_6 for the monomer and k_7 for the dimer. With these recombinations included here, too, it is possible to simulate the decay for the monomer and dimer ions (after the electron beam has stopped and thus a constant initial amount of RIP ions has been established) qualitatively correctly (Figures 4 and 5). The calculated monomer curves decay a little too slowly, while the dimer curves decay a little too fast. But the relative similarity of the concentration dependence is clearly visible. The differences occur probably as a result of non-optimal choice of rate constants and initial conditions, e.g., how many monomer ions are already formed during the RIP ions' ionization process. The goal of this model is, however, not to reach absolute accuracy, but to help determine what is responsible for the signal decay. Together with the experimental facts (and the fact that, with increasing k_6 and k_7 in order to simulate stronger electric fields, a qualitatively correct change of the decay curves towards faster decays is obtained with help of this model) it seems to be evident that the signal decay is indeed based on recombination reactions (but with the role that the electrical field plays in the decay still not fully understood). Thus the parameters obtained from the decay curves are caused by a different effect which is independent from the drift behavior of the analyte ions. These parameters are orthogonal parameters with respect to the reduced mobility, supporting the summary that the amount of analytic information available with pulsed IMS is increased.

Conclusion and outlook

Pulsed electron sources used in ion mobility spectrometry have experienced a drastic change in purpose. Initially only seen as a non-radioactive alternative that uses less energy than a continuously operating source, they (i.e., IMS devices using a pulsed electron gun, since there are no published results of any further development of using the pulsed corona discharge after 2005) now offer improvement regarding the analytical information this detector family can provide. Enhancement in selectivity, improved identification power and quantitative analysis possible in the lower ppb range in addition to the reduced mobility are the benefits that can be obtained with pulsed ion mobility spectrometers by using the decay characteristic of signals, while the standard IMS device offers only the analyte's reduced mobility. Therefore the main disadvantages of IMS devices are reduced regarding their performance limitation for field operation. Employing the signal decay characteristic is still in its developmental phase, and further parameters that can be extracted from the signal decay and its dependencies are likely to be found.

The main control parameter when using the signal decay is the delay time between ionization and ion detection. So only the possibility to stop the electron beam at any time is used. However, the electron pulse has more controllable parameters, e.g., duration and intensity. One area yet to be investigated is the behavior of signals when using very short ionization pulses. For the decay behavior the pulse length and intensity were chosen so that a sufficiently strong signal was obtained. Very short ionization pulses could allow for a shift of the chemical reactions from thermodynamic reaction control to kinetic reaction control by just not giving the system enough time to reach the thermodynamic equilibrium. Thus a direct influence on the composition of the reaction product mixture could be possible. This possibility would be beneficial when competing reaction pathways do not allow the detection of a certain analyte in the presence of a certain other analyte. A typical example is the the oil industry, which is a very demanding sector for a large variety of detectors. With standard IMS devices it is very difficult to detect, e.g., benzene in the presence of even smallest amounts of toluene, i.e., toluene would always the dominant signal (because of its proton affinity the charge exchange reactions would finally end with the formation of toluene ions with almost no benzene ions left to be detected). Using a very short electron pulse and immediate extraction of the ions from the reaction region could then possibly lead to a better benzene signal. The pulsed electron beams have already led to significant improvements, but still there are many unknown territories to discover. It remains interesting to see how and which new doors will be opened with the help of pulsed ion mobility spectrometry.

Received May 21, 2012; accepted June 15, 2012; previously published online July 26, 2012

References

An, Y.; Aliaga-Rossel, A.; Choi, P.; Gilles, J.-P. Development of a short pulsed corona discharge ionization source for Ion Mobility Spectrometry. *Rev. Sci. Instr.* **2005**, *76*, 085105 (6 pages).

Armenta, S.; Alcala, M.; Blanco, M. A review of recent, unconventional applications of ion mobility spectrometry (IMS). *Anal. Chim. Acta* **2011**, *703*, 114–123.

Asbury, G. R.; Klasmeier, J.; Hill, H. H. Jr. Analysis of explosives using electrospray ionization/ion mobility spectrometry (ESI/IMS). *Talanta* **2000**, *56*, 1291–1298.

Baether, W.; Zimmermann, S.; Gunzer, F. Investigation of the influence of voltage parameters on decay times in an ion mobility spectrometer with a pulsed non-radioactive electron source. *Int. J. Ion. Mobil. Spectrom.* **2010**, *13*, 95–101.

Baether, W.; Zimmermann, S.; Gunzer, F. Pulsed ion mobility spectrometer for the detection of toluene 2,4-diisocyanate in ambient air. *IEEE Sens. J.* **2012a**, *12*, 1748–1754.

Baether, W.; Zimmermann, S.; Gunzer, F. Quantitative information in decay curves obtained with a pulsed ion mobility spectrometer. *Analyst* **2012b**, *137*, 2723–2727.

Barnett, D. A.; Oullette, R. J. Elimination of the helium requirements in high-field asymmetric waveform ion mobility spectrometry (FAIMS): beneficial effects of decreasing the analyzer gap width on peptide analysis. *Rapid Commun. Mass Spectrom.* **2011**, *25*, 1959–1971.

Boger, Z.; Karpas, Z. Use of neural networks for quantitative measurements in ion mobility spectrometry (IMS). *J. Chem. Inf. Comput. Sci.* **1994**, *34*, 576–580.

Borsdorf, H.; Rudolph, M. Gas-phase ion mobility studies of constitutional isomeric hydrocarbons using different ionization techniques. *Int. J. Mass Spectrom.* **2001**, *208*, 67–72.

Borsdorf, H.; Mayer, T.; Zarejousheghani, M.; Eiceman, G.A. Recent developments in ion mobility spectrometry. *Appl. Spec. Rev.* **2011**, *46*, 472–521.

Bradbury, N. E.; Nielsen, R. A. Absolute values of the electron mobility in hydrogen. *Phys. Rev.* **1936**, *5*, 388–393.

Brokenshire, J. L.; Dharmarajan, V.; Coyne, L. B.; Keller, J. J. Near real time monitoring of TDI vapour using ion mobility spectrometry (IMS). *J. Cell. Plastics* **1990**, *26*, 123–142.

Chen, Y. H.; Siems, W. F.; Hill, H. H. Jr. Fourier transform electrospray ion mobility spectrometry. *Anal. Chim. Acta* **1996**, *334*, 75–84.

Chiarello-Ebner, K. Pursuing efficiency: new developments in cleaning technology. *Pharm. Techn. Pharm. Technol.* **2006**, *30*, 52–64.

Clark, A.; Arnold, P. D.; Brittain, A. H.; Wilson, R. C. The use of pulsed corona discharge ionization in high temperature IMS systems. Paper, Sixth International Workshop on Ion Mobility Spectrometry; Bastei, Germany, 1997.

Cochems, P.; Gunzer, F.; Langejuergen, J.; Heptner, A.; Zimmermann, S. Selective ion suppression as a pre-separation method in ion mobility spectrometry using a pulsed electron gun. *Int. J. Ion Mobil. Spectrom.* **2012**, *15*, 31–39.

Davis, E. J.; Dwivedi, P.; Tam, M.; Siems, W. F.; Hill, H. H. High pressure ion mobility spectrometry. *Anal. Chem.* **2009**, *81*, 3270–3275.

Djidja, M. C.; Claude, E.; Snell, M. F.; Scriven, P.; Francese, S.; Carolan V. A.; Clench, M. R. MALDI-ion mobility separation-mass spectrometry imaging of glucose-regulated protein 78 kDa (Grp 78) in human formalin fixed paraffin embedded pancreatic adenocarcinoma tissue sections. *J. Proteome Res.* **2009**, *8*, 4876–4884.

Eckers, C.; Laures, A. M.-F.; Giles, K.; Major, H.; Pringle, S. Evaluating the utility of ion mobility separation in combination with high-pressure liquid chromatography/mass spectrometry to facilitate detection of trace impurities in formulated drug products. *Rapid Commun. Mass Spectrom.* **2007**, *21*, 1255–1263.

Eiceman, G. A. Ion mobility as a fast monitor of chemical composition. *Trends Anal. Chem.* **2002**, *21*, 259–275.

Eiceman, G. A.; Karpas, Z. Ion mobility spectrometry; CRC Press: Boca Raton, USA, 2005.

Ewing, R. G.; Eiceman, G. A.; Stone, J. A. Proton bound cluster ions in ion mobility spectrometry. *Int. J. Mass Spectrom.* **1999**, *193*, 57–68.

Ewing, R. G.; Atkinson, D. A.; Eiceman, G. A.; Ewing, G. J. A critical review of ion mobility spectrometry for the detection of explosives and explosive related compounds. *Talanta* **2001**, *54*, 515–529.

Fraga, C. G.; Kerr, D. R.; Atkinson, D. A. Improved quantitative analysis of ion mobility spectrometry by chemometric multivariate calibration. *Analyst* **2009**, *134*, 2329–2337.

Garofolo, F.; Marziali, F.; Migliozzi, V.; Stama, A. Rapid quantitative determination of 2,4,6-trinitrotoluene by ion mobility spectrometry. *Rapid Commun. Mass Spectrom.* **1996**, *10*, 1321–1326.

Guharay, S. K.; Dwivedi, P.; Hill, H. H. Jr. Ion mobility spectrometry: ion source development and applications in physical and biological Sciences. *IEEE Trans. Plasma Sci.* **2008**, *36*, 1458–1470.

Gunzer, F.; Ulrich, A.; Baether, W. A novel non-radioactive electron source for ion mobility spectrometry. *Int. J. Ion Mobil. Spectrom.* **2010a**, *13*, 9–16.

Gunzer, F.; Zimmermann, S.; Baether, W. Application of a nonradioactive pulsed electron source for ion mobility spectrometry. *Anal. Chem.* **2010b**, *82*, 3756–3763.

Gunzer, F.; Baether, W.; Zimmermann, S. Investigation of dimethyl methyl-phosphonate (DMMP) with an ion mobility spectrometer using a pulsed electron source. *Int. J. Ion Mobil. Spectrom.* **2011**, *14*, 99–107.

Han, H.-Y.; Huang, G.-D.; Jin, S.-P.; Zheng, P.-C.; Xu, G.-H.; Li, J.-Q.; Wang, H.-M.; Chu, Y.-N. Determination of alcohol compounds using corona discharge ion mobility spectrometry. *J. Env. Sci. China* **2007**, *19*, 751–756.

Harris, G. A.; Nyadong, L.; Fernandez, F. M. Recent developments in ambient ionization techniques for analytical mass spectrometry. *Analyst* **2008**, *133*, 1297–1301.

Hill, C. A.; Thomas, C. L. P. Pulsed corona discharge: a replacement for 63Ni in ion mobility spectrometry? *Int. J. Ion Mobil. Spectrom.* **2002**, *5*, 155–160.

Hill, C. A.; Thomas, C. L. P. A pulsed corona discharge switchable high resolution ion mobility spectrometer-mass spectrometer. *Analyst* **2003**, *128*, 55–60.

Hill, C. A.; Thomas, C. L. P. Programmable gate delayed ion mobility spectrometry-mass spectrometry: a study with low concentrations of dipropylene-monomethyl-ether in air. *Analyst* **2005**, *130*, 1155–1161.

Jafari, M. T.; Rezaei, B.; Javaheri, M. A new method based on electrospray ionization ion mobility spectrometry (ESI-IMS) for simultaneous determination of caffeine and theophylline. *Food Chem.* **2011**, *126*, 1964–1970.

Jazan, E.; Tabrizchi, M. Kinetic study of proton-bound dimer formation using ion mobility spectrometry. *Chem. Phys.* **2009**, *355,* 37–42.

Khayamian, T.; Tabrizchi, M.; Taj, N. Direct determination of ultra-trace amounts of acetone by corona-discharge ion mobility spectrometry. *Fresenius J. Anal. Chem.* **2001**, *370*, 1114–1116.

Khayamian, T.; Tabrizchi, M.; Jafari, M. T. Corona discharge ion mobility spectrometry. *Talanta* **2003**, *59*, 327–333.

Khayamian, T.; Tabrizchi, M.; Jafari, M. T. Quantitative analysis of morphine and noscapine using corona discharge ion mobility spectrometry with ammonia reagent gas. *Talanta* **2006**, *69*, 795–799.

Klaassen, T.; Szwandt, S.; Kapron, J. T. Validated quantitation method for a peptide in rat serum using liquid chromatography/high field asymmetric waveform ion mobility spectrometry. *Rapid Commun. Mass Spectrom.* **2009**, *23*, 2301–2306.

Krueger, C. A.; Hilton, C. K.; Osgood, M.; Wu, J.; Wu, C. High resolution electrospray ionization ion mobility spectrometry. *Int. J. Ion Mobil. Spectrom.* **2009**, *12*, 33–37.

Liu, X.; Valentine, S. J.; Plasencia, M. D.; Trimpin, S.; Naylor, S.; Clemmer, D. E. Mapping the human plasma proteome by SCX-LC-IMS-MS. *J. Am. Soc. Mass Spectrom.* **2007**, *18*, 1249–1264.

Makinen, M. A.; Anttalainen, O. A.; Sillanpää, M. Ion mobility spectrometry and its applications in detection of chemical warfare agents. *Anal. Chem.* **2010**, *82*, 9594–9600.

Makinen, M.; Sillanpää, M.; Vitaanen, A. K.; Knap, A.; Mäkelä, J. M.; Puton, J. The effect of humidity on sensitivity of amine detection in ion mobility spectrometry. *Talanta* **2011**, *84*, 116–121.

Matsaev, V.; Gumerov, M.; Krasnobaev, L.; Pershenkov, V.; Belyakov, V.; Christyakov, A.; Boudovitch, V. IMS spectrometers with radioactive, X-ray, UV and laser ionization. *Int. J. Ion. Mobil. Spectrom.* **2002**, *5*, 112–114.

McDaniel, E. W.; Mason, A. E. The mobility and diffusion of ions in gases; John Wiley & Sons: New York, USA, 1973.

McLean, J. A.; Ridenour, W. B.; Caprioli, R. M. Profiling and imaging of tissues by imaging ion mobility-mass spectrometry. *J. Mass Spectrom.* **2007**, *42*, 1099–1105.

McMinn, D. G.; Kinzer, J. A.; Shumate, C. B.; Siems, W. F.; Hill, H. H. Jr. Ion mobility detection following liquid chromatography separation. *J. Microcol.* **1990**, *2*, 188–192.

Morozov, A.; Krücken, R.; Ulrich, A.; Wieser, J. Spatial distribution of fluorescent light emitted from neon and nitrogen excited by low energy electron beams. *J. Appl. Phys.* **2006**, *100*, 093305.

Morozov, A.; Heindl, T.; Wieser, J.; Krücken, R.; Ulrich, A. Transmission of ~10 keV electron beams through thin ceramic foils: measurements and Monte Carlo simulations of electron energy distribution functions. *Eur. Phys. J. D* **2008a**, *46*, 51–57.

Morozov, A.; Heindl, T.; Wieser, J.; Krücken, R.; Ulrich, A. Conversion efficiencies of electron energy to vacuum ultraviolet light for Ne, Ar, Kr and Xe excited with continuous electron beams. *J. Appl. Phys.* **2008b**, *103*, 103301.

Mühlberger, F.; Streibel, T, Wieser, J.; Ulrich, A.; Zimmermann, R. Single photon ionization time-of-flight mass spectrometry with a pulsed electron beam pumped excimer VUV lamp for on-line gas analysis: setup and first results on cigarette smoke and human breath. *Anal. Chem.* **2005**, *77*, 7408–7414.

Mulugeta, M.; Wibetoe, G.; Engelsen, C. J.; Lund. W. Analyses of biogenic amines using corona discharge ion mobility spectrometry. *Talanta* **2010**, *78*, 1081–1087.

Oberhüttinger, C.; Langmeier, A.; Oberpriller, H.; Kessler, M.; Goebel, J.; Müller,G. Hydrocarbon detection using laser ion mobility spectrometry. *Int. J. Ion. Mobil. Spectrom.* **2009**, *12*, 23–32.

Politis, A.; Park. A. Y.; Hyung, S.-J.; Barsky, D.; Ruotolo, B. T.; Robinson, C. V. Integrating ion mobility mass spectrometry with molecular modeling to determine the architecture of multiprotein complexes. *PloS ONE* **2010**, *5*, e12080.

Poziomek, E. J.; Eiceman, G. A. Solid-phase enrichment, thermal desorption, and ion mobility spectrometry for field screening of organic pollutants in water. *Environ. Sci. Technol.* **1992**, *26*, 1313–1318.

Roehl, J. E. Environmental and process applications for ion mobility spectrometry. *Appl. Spectros. Rev.* **1991**, *26*, 1–57.

Ruotolo, B. T.; Benesch, J. L. P.; Sandercock, A. M.; Hyung, S.-J.; Robinson, C. V. Ion-mobility-mass spectrometry analysis of large protein complexes. *Nature Protocols* **2008**, *3*, 1139–1152.

Schmidt, H.; Baumbach, J. I.; Sielemann, S.; Wember, M.; Klockow, D. Is partial discharge ion mobility spectrometry an effective tool for the sensitive determination of halogenated hydrocarbons? *Int. J. Ion. Mobil. Spectrom.* **2001**, *4*, 39–42.

Schneider, B. B.; Covey, T. R.; Coy, S. L.; Krylov, E. V.; Nazarov. E. G. Control of chemical effects in the separation process of a differential mobility mass spectrometer system. *Eur. J. Mass Spectrom.* **2010**, *16*, 57–71.

Shvartsburg, A. A.; Tang, K.; Smith, R. D.; Holden, M.; Rush, M.; Thompson, A.; Toutoungi, D. Ultrafast differential ion mobility spectrometry at extreme electric fields coupled to mass spectrometry. *Anal. Chem.* **2009**, *81*, 8048–8053.

Sielemann, S.; Baumbach, J. I.; Schmidt, H. IMS with non-radioactive ionization sources suitable to detect chemical warfare agent simulation substances. *Int. J. Ion Mobil. Spectrom.* **2002**, *5*, 143–148.

Steiner, W. E.; Klopsch, S. J.; English, W. A.; Clowers, B. H.; Hill, H. H. Jr. Detection of a chemical warfare simulant in various aerosol matrices by ion mobility time-of-flight mass spectrometry. *Anal. Chem.* **2005**, *77*, 4792–4799.

Tabrizchi, M.; Ilbeigi, V. Detection of explosives by positive corona discharge ion mobility spectrometry. *J. Hazard. Mat.* **2010**, *176*, 692–696.

Tabrizchi, M.; Khayamian, T.; Taj, N. Design and optimization of a corona discharge ionization source for ion mobility spectrometry. *Rev. Sci. Instr.* **2000**, *7*, 2321–2328.

Tang, X.; Bruce, J. E.; Hill, H. H. Jr. Characterizing electrospray ionization using atmospheric pressure ion mobility spectrometry. *Anal. Chem.* **2006**, *78*, 7751–7760.

Waltman, M. J.; Dwivedi, P.; Hill, H. H. Jr, Blanchard, W. C.; Ewing, R. G. Characterization of a distributed plasma ionization source (DPIS) for ion mobility spectrometry and mass spectrometry. *Talanta* **2008**, *77*, 249–255.

Wieser, J.; Murnick, D. E.; Ulrich, A.; Huggins, H. A.; Liddle, A.; Brown, W. L. Vacuum ultraviolet rare gas excimer light source. *Rev. Sci. Instrum.* **1997**, *68*, 1360–1365.

Wittmer D. K.; Chen, Y. H.; Luckenbill, B.; Hill, H. H. Jr. Electrospray ionization ion mobility spectrometry. *Anal. Chem.* **1994**, *66*, 2348–2355.

Wu, C.; Siems, W. F.; Hill, H. H. Jr. Secondary electrospray ionization ion mobility spectrometry – mass spectrometry of illicit drugs. *Anal. Chem.* **2000**, *72*, 396–403.

Wüthrich, B. Adverse reactions to food additives. *Ann. Allergy* **1993**, *71*, 379–384.

Xu, J.; Whitten, W. B.; Lewis, T. A.; Ramsey, J. M. A miniature ion mobility spectrometer with a pulsed corona discharge ion source. *Int. J. Ion Mobil. Spectrom.* **2001**, *4*, 3–6.

Xu, J.; Whitten, W. B.; Ramsey, J. M. Pulsed-ionization miniature ion mobility spectrometer. *Anal. Chem.* **2003**, *75*, 4206–4210.

Yamagaki, T.; Sato, A. Isomeric oligosaccharides analyses using negative-ion electrospray ionization ion mobility spectrometry combined with collision-induced dissociation MS/MS. *Anal. Sci.* **2009**, *25*, 985–988.

Zheng, P.; Harrington, P. B.; Davis, D. M. Quantitative analysis of volatile organic compounds using ion mobility spectrometry and cascade correlation neural networks. *Chemometr. Intell. Lab.* **1996**, *33*, 121–132.

Wolfgang Baether received the Diploma degree in organic chemistry in 1980. He received the Doctoral degree from the University of Bielefeld, Germany, in 1984. His Doctoral thesis was in the field of organic mass spectrometry. In 1984, he joined the Drägerwerk AG & Co. KGaA, Luebeck, Germany. His work focused on detector tube development. In 1989, he became Head of the Tube Development and Application Technology Department. In 1998, he joined the Draeger Research Group as a Technology Scout for gas measuring technologies based on ionization in the gas phase with a focus on ion mobility spectrometry.

Stefan Zimmermann received his Diploma in electrical engineering in 1996 and his PhD in electrical engineering in 2001 from the Technical University Hamburg-Harburg, Germany. He was with the Department of Microsystems Technology at the Technical University Hamburg-Harburg from 1996 to 2001. His research focused on MEMS design and fabrication. In 2001, he joined the Berkeley Sensor and Actuator Center, University of California, Berkeley, as a Postdoctoral Research Engineer with support of a Feodor-Lynen Fellowship of the Alexander von Humboldt Foundation. His research focused on BioMEMS and the development of a disposable continuous glucose monitor. In 2004, he joined the Research Unit of Dräger, Luebeck, Germany, where he worked on MEMS for medical and safety applications. His latest position at Dräger was head of Chemical and Biochemical Sensors. In 2009 he joined the Leibniz University Hannover, Germany as a full professor in sensors and measurement technology. His current research is focused on the development of sensors and nanosensors for ultrasensitive trace gas detection.

Frank Gunzer received his Diploma in physics in 1999 and the Doctoral degree in 2003 from the Christian-Albrecht-University in Kiel, Germany. The Doctoral thesis was in the field of laser mass spectrometry. In 2003 he joined the German University in Cairo, where he is currently employed as an associate professor in the Faculty of Information Engineering and Technology. His research is focused on the detection and analysis of substances with help of different spectroscopy and spectrometry techniques supported by computer algorithms. Since 2011 he has been the head of the Electronics Department of the Faculty of Information Engineering and Technology.